

Lasers in Manufacturing Conference 2019

# Laser material processing and functionalization with tailored focal intensity distributions

Anna Möhl<sup>a</sup>, Frank A. Müller<sup>b</sup>, Ulrike Fuchs<sup>a\*</sup>, Stephan Gräf<sup>b</sup>

<sup>a</sup> asphericon GmbH, Stockholmer Str. 9, 07747 Jena

<sup>b</sup> Otto Schott Institute of Materials Research (OSIM), Friedrich Schiller University, Löbdergraben 32, 07743 Jena, Germany

---

## Abstract

Gaussian intensity profiles are widely used in the field of laser material processing. Nevertheless, there are applications, where the inhomogeneous beam profile is not acceptable, and another intensity distribution would be much more advantageous. We show that refractive beam shaping systems provide very good results for generating tailored focal intensity distributions, e.g. top-hat or doughnut shaped profiles. Even though using just one beam shaping system the width of the profiles is scalable. Beyond, the device is suitable for working with a scanner and F-Theta lens as commonly used for material processing. Results of material processing of stainless steel are presented for different focal intensity distributions and evaluated. In conclusion, the optimization of processing time and parameters are discussed. Additionally, an application example is presented in which laser-induced periodic surface structures (LIPSS) are generated that can be used for the functionalization of surfaces.

Keywords: Beam Shaping, Laser material processing, surface functionalization, cutting, drilling

---

## 1. Introduction

Due to their flexibility, Gaussian intensity profiles are widely used, especially in the field of laser material processing. Nevertheless, there are some applications, where a Gaussian profile is not ideal for all processing tasks. The inhomogeneous beam profile and the energy loss at the edge of the beam might not be acceptable. Other intensity distributions might be much more suitable. It could be shown that refractive beam shaping systems provide very good results for generating tailored focal intensity distributions, e.g. top-

---

\* Corresponding author. Tel.: +49 3641 3100 500.  
E-mail address: u.fuchs@asphericon.com.

hat or donut shaped profiles. This is mainly caused by their high efficiency and flexibility (with respect to wavelength changes), their simple structure and consequently, their good manufacturability.

Therefore, it is subject of this work to introduce a very compact and flexible refractive, aspheric beam shaping solution for material processing. The input intensity distribution is a collimated Gaussian beam profile, which is transformed into a collimated Bessel-like and a focused top-hat intensity distribution, respectively. The system enables smooth integration into existing set-ups. It is possible to use it with a collimated laser beam or a fiber-coupled source. Furthermore, the input and output beam are scalable, so that a wide range of top-hat and donut widths can be covered with just one beam shaper. Beyond, the device is suitable for working with a scanner and F-Theta lens as commonly used for material processing.

In this work, selected design investigations as well as results of the practical testing are presented. For the latter, some investigations were carried out using a Yb:KYW thin disc fs-laser on stainless steel to prove the functionality and to evaluate the processing results. Additionally, an application example is presented in which laser-induced periodic surface structures (LIPSS) are generated that can be used for the functionalization of surfaces.

## 2. Generating Taylored focal intensity distributions

To obtain a focused top-hat intensity distribution a known approach, based on diffraction theory and Fourier transform correlation, was chosen [1, 2]. It is assumed, that a simple lens performs a Fourier transform on the input intensity function and the corresponding Fourier counterpart occurs in its focal plane. That means, to generate a focused top-hat intensity distribution, which can be described by a circ-function, the resulting input intensity function must be a collimated Bessel-sinc shaped intensity profile. The theoretical background of this phenomenon is discussed several times in literature [1, 2]. Since a collimated Gauss to focused top-hat intensity transformation was initially desired, a further beam shaping step from collimated Gaussian to collimated Bessel-sinc beam profile is necessary. This can be done with the help of a phase plate, as described in [3]. The phase plate has a binary structure with an increased central part, based on a known patent system [3]. The principle layout of the beam shaping unit is shown in Figure 1.

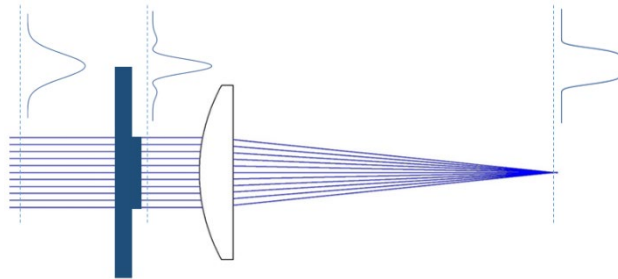


Fig. 1. Principle layout of the focused beam shaping system, consisting of beam shaping element and focusing optics, with important intensity distributions (ray distributions in front and behind the phase plate are not displayed correctly due to ray tracing).

In practice, beam shaping is a complex process, especially if a beam shaping system should be added in an existing set-up. There are two aspects, which should be considered. The first is the adaption of the system input to the laser source and the second is the adaption of the system output to the individual set-up. What is needed is a design, that can handle both tasks. Due to the high flexibility of beam shaping system it is possible not only to use it in combination with a collimated laser beam, but to use it with a fiber-coupled source. For this, just some a|BeamExpanders for the appropriate magnification and a a|AspheriColl

are needed. The system output is perfectly adaptable, since the size of the top-hat beam profile is scalable by the focal length of a focusing lens. So nearly arbitrary dimensions of top-hat beam profiles can be generated. An exemplary layout of the discussed configuration is shown in Figure 2.

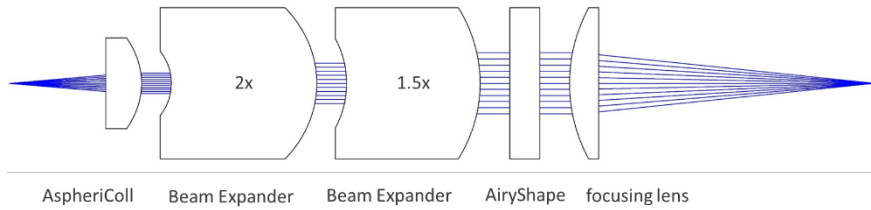


Fig.2. Flexible adaption of input and output beam diameter of the focused beam shaping system (a|AiryShape).

According to the working principle of the beam shaping system, it is possible, not just to generate one top-hat beam profile in the focal plane of a focusing lens but create different beam profiles in different working distances. There is no need for additional components in the system set-up. In Figure 3 normalized beam profile sections along its propagation direction (z-axis) are summarized in one diagram. The detected range is  $\pm 1.5$  mm around the waist location. Furthermore, the corresponding most interesting intensity profiles in the different working planes are shown, too.

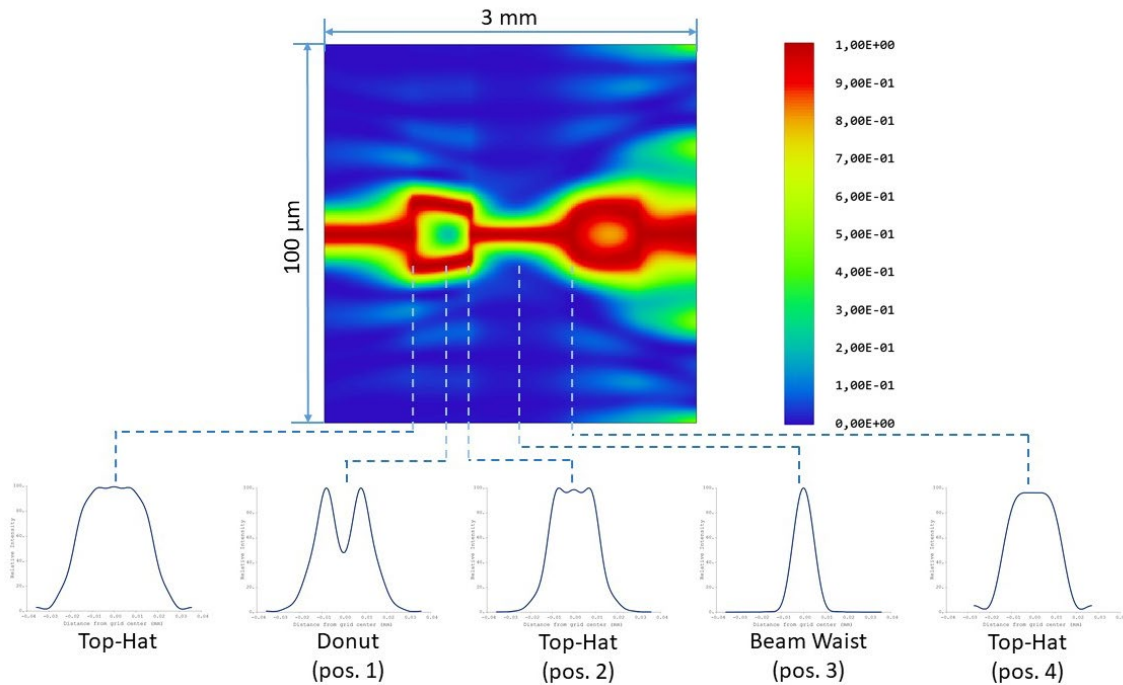


Fig. 2. Visualization of normalized beam profiles along the z-direction in a range of  $\pm 1.5$  mm around the focal plane and corresponding beam profiles for the different planes.

### 3. Practical testing of the beam shaping element

The practical testing of the beam shaping element was carried out with the experimental setup schematically illustrated in Figure 4. A diode pumped Yb:KYW thin disc fs-laser system (JenLas D2.fs, Jenoptik, Germany) was used as radiation source delivering linearly polarized laser pulses at the central wavelength  $\lambda = 1025$  nm with a pulse duration  $\tau = 300$  fs (FWHM) and pulse energies  $E_{\text{imp}} \leq 40$   $\mu\text{J}$  at a repetition frequency  $f_{\text{rep}} = 100$  kHz. The shaping of the Gaussian output beam ( $M^2 \sim 1.08$ ) was realized by a beam expander (5x) and the a|AiryShape according to Figure 2. The laser beam was focused by using a galvanometer scanner (IntelliScan14, Scanlab, Germany) including a f-Theta objective (JENar, Jenoptik, Jena, Germany) with a focal length  $f_L = 100$  mm.

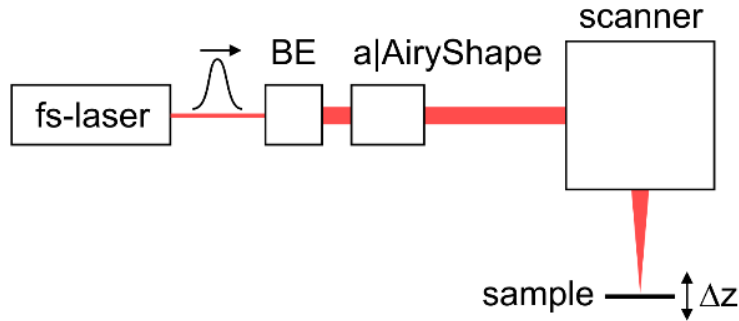


Fig. 4. Experimental setup for practical testing of the beam shaping element (a|AiryShape); BE: beam expander (5x).

Commercially available austenitic stainless steel (X2CrNiMo17-12-2, Outokumpu, Germany) was used as substrate material. The sample surface was manually grounded and polished to a mirror finish with an average surface roughness  $R_a \sim 4$  nm using SiC abrasive paper of 800, 1200 and 2400 grit and 6  $\mu\text{m}$ , 3  $\mu\text{m}$  and 1  $\mu\text{m}$  polycrystalline diamond suspension, respectively. The laser processed sample surfaces were ultrasonically cleaned in acetone and isopropanol and subsequently characterized by scanning electron microscopy (SEM) (SigmaVP, Carl Zeiss, Germany) at an accelerating voltage of 5 kV using a secondary electron detector.

The adequate function of the beam shaping element was proven by single spot experiments using the specific beam profiles provided by the a|AiryShape (pos. 1-4 in Figure 3). For this purpose, the material surface was placed under the focusing optic at a certain z-position and ablation spots with a different number  $N$  of fs-laser pulses were fabricated at a fixed pulse energy  $E_{\text{imp}} = 13$   $\mu\text{J}$ . In the beam waist (pos. 3), the focal spot diameter was determined to be  $2w_f \sim 34$   $\mu\text{m}$  ( $1/e^2$ -intensity) using the method proposed by Liu [4]. This results in a laser peak fluence  $F = 2E_{\text{imp}}/(\pi w_f^2) = 2.8$  J/cm<sup>2</sup> in the beam waist. Figure 5 shows the corresponding SEM micrographs of the stainless-steel surface obtained from irradiating the surface at normal incidence and under ambient air. As was to be expected, the ablation depth increases with increasing number of pulses. It becomes evident that all ablation spots exhibit characteristic nanostructures. These so-called laser-induced periodic surface structures (LIPSS) are of particular interest for the engineering of functional material surfaces with e.g. outstanding optical and tribological properties [5]. Their origin has already been described in numerous works on stainless steel [6, 7]. In this context it was shown that LIPSS on metals are characterized by a spatial period in the order of the utilized laser wavelength and an orientation perpendicular to the linear beam polarization (Figure 5j).

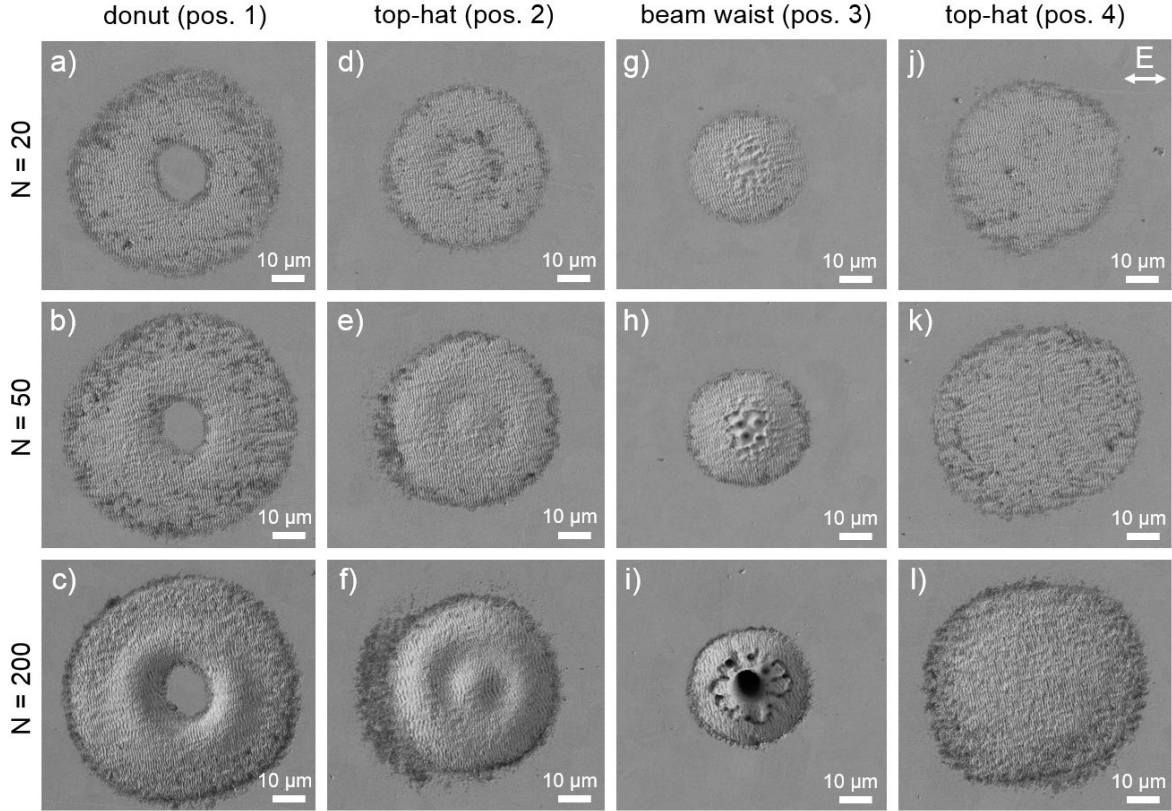


Fig. 5. SEM micrographs of the stainless-steel surface upon irradiation with the specific beam profiles provided by the a|AiryShape along the z-direction as a function of the laser pulse number  $N$  using a pulse energy  $E_{\text{imp}} = 13 \mu\text{J}$ . The linear beam polarisation is indicated in (j) by the direction of the electrical field vector  $E$ .

Based on Figure 5, the present study demonstrates a good agreement between the theoretical beam shaping simulation and the laser processing experiments. This is particularly expressed in the following points:

- The ablation spot produced with the donut-shaped intensity profile in position 1 is characterised by a well-pronounced intensity minimum in the centre where the material surface kept unaffected by the laser irradiation (Figure 5a-c).
- The slight intensity modulation in the plateau of the top-hat in position 2 is reflected in the surface topography of the ablation spot produced with  $N = 200$  pulses (Figure 5f).
- In the beam waist in position 3, typical phenomena related to the high intensive centre of the Gaussian beam profile caused by heat accumulation and melt formation (Figure 5g, h) as well as excessive ablation (Figure 5i) can be observed. This concerns in particular the very inhomogeneous ablation within the ablation crater.

- The unmodulated, flat plateau of the top-hat in position 4 is characterized by a homogeneous ablation over the beam cross-section, which is also expressed in the homogeneity of the occurring LIPSS pattern (Figure 5j-l).

The transfer of functional properties based on LIPSS to industrial applications requires in most cases large surface areas structured with LIPSS. This is realized by a bidirectional scanning of the surface with a lateral spacing  $\Delta x$  between two adjacent scan lines. In this context, top-hat intensity profiles as provided by the a|AiryShape offer the possibility to achieve a more homogeneous energy deposition on the material surface and thus highly regular LIPSS. Figure 6 shows a LIPSS pattern that was produced with a scanning velocity  $v = 0.67$  m/s, a lateral spacing  $\Delta x = 6$   $\mu\text{m}$  and a pulse energy  $E_{\text{imp}} = 13$   $\mu\text{J}$  using the top-hat beam profile in position 4. Taking into account the ablation diameter of about 47  $\mu\text{m}$  obtained from Figure 5j ( $N = 20$ ), the ablation spot area is effectively hit by approximately 40 pulses during scanning. The generated grating-like structures consist of highly regular LIPSS oriented perpendicular to the linear polarization. The micrograph reveals that the LIPSS can be coherently written over a large area despite the line-wise scanning process. The homogeneity of the grating with respect to the spatial period and the orientation can be quantitatively described by the 2D-Fourier transform of the SEM micrograph (inset in Figure 6). Consequently, the spatial period of the LIPSS was determined to  $(940 \pm 30)$  nm. Beyond, the cross section of the Fourier spectrum demonstrates that the spatial period is limited to a very narrow range, which corresponds to a very high homogeneity. In addition, the corresponding dispersion of the LIPSS orientation angle was calculated to  $\delta\theta \sim 9^\circ$ , which emphasises the well-defined alignment of the grating-like structures [8].

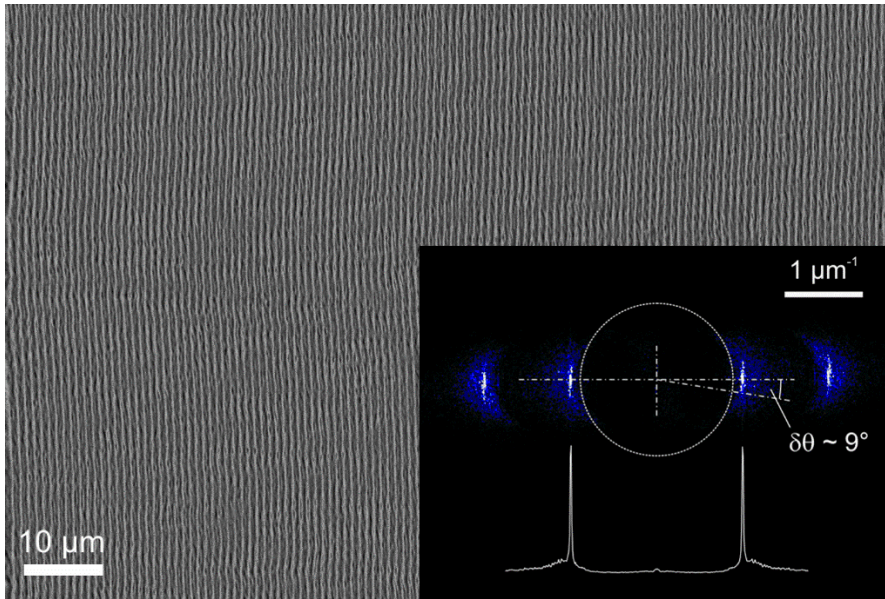


Fig. 6. SEM micrograph demonstrating the large-area structuring of stainless steel with LIPSS using the top-hat beam profile in position 4. The inset corresponds to the 2D-Fourier transform of the SEM micrograph,  $\delta\theta$  represents the dispersion of the LIPSS orientation angle, the utilized laser wavelength  $\lambda = 1025$  nm is represented by the dotted circle, and curve in the bottom shows the cross section of the 2D-Fourier spectrum.

#### 4. Conclusion

The efficiency of a laser process or a specific application can be improved in many ways. Changing the intensity distribution of the working laser beam is one effective parameter in order to achieve optimum system performance. In this paper a compact refractive beam shaping element is introduced, which generates certain tailored intensity distributions in combination with a focusing optics.

Furthermore, this beam shaping element was tested practically in a laser set-up suitable for laser material processing. It was shown, that there is a good agreement between the theoretical beam shaping simulation and the laser processing experiments. In addition, an example was presented in which laser-induced periodic surface structures (LIPSS) are generated using the introduced beam shaping element. These surface structures were analysed with respect to their spatial period. As a result, very homogeneous grating-like structures were generated.

#### References

- [1] Goodman, J. W., Introduction to Fourier Optics, 3rd Edition, Englewood: Roberts & Comapany, 2005.
- [2] Dickey, F. M., Laser Beam Shaping - Theory and Techniques, 2nd Edition, Boca Raton: CRC Press, 2014.
- [3] J. J. Cordingley, „Method for Serving Integrated-Circuit Connection Paths by a Phase-Plate-Adjusted Laser Beam“. US Patent 5300756, 5 April 1994.
- [4] Liu, J.M., „Simple Techniques for Measurement of Pulsed Gaussian-beam Spot Sizes,“ *Opt. Lett.* 7, pp. 196- 198, 1982.
- [5] Müller, F.A., Kunz, C., Gräf, S., „Bio-inspired functional surfaces based on laser-induced periodic surface structures,“ *Materials* 9, p. 476, 2016.
- [6] Gräf, S., Müller, F.A., „Polarisation-dependent generation of fs-laser induced periodic surface structures,“ *Appl. Surf. Sci.* 331, pp. 150-155, 2015.
- [7] Gräf, S., Kunz, C., Undisz, A., Wonneberger, R., Rettenmayr, M., Müller, F.A., „Mechano-responsive colour change of laser-induced periodic surface structures,“ *Appl. Surf. Sci.* 471, pp. 645-651, 2019.
- [8] Gnilytskyi, I., Derrien, T.J.Y., Levy, Y., Bulgakova, N.M., Mocek, T., Orazi, L., „High-speed manufacturing of highly regular femto-second laser-induced periodic surface structures: Physical origin of regularity,“ *Sci. Rep.* 7, p. 8485, 2017.